

RESEARCH LETTER

10.1002/2015GL067545

Key Points:

- The Brewer-Dobson circulation is rising in response to greenhouse gas forcing
- The rise in the circulation causes an increase in the mass flux at any given pressure level
- The actual mass exchange between stratosphere and troposphere, however, changes little

Correspondence to:

S. Oberländer-Hayn,
sophie.oberlaender@met.fu-berlin.de

Citation:

Oberländer-Hayn, S., et al. (2016), Is the Brewer-Dobson circulation increasing or moving upward?, *Geophys. Res. Lett.*, 43, doi:10.1002/2015GL067545.

Received 23 DEC 2015

Accepted 3 FEB 2016

Accepted article online 6 FEB 2016

Is the Brewer-Dobson circulation increasing or moving upward?

Sophie Oberländer-Hayn¹, Edwin P. Gerber², Janna Abalichin¹, Hideharu Akiyoshi³, Andreas Kerschbaumer^{1,4}, Anne Kubin^{1,5}, Markus Kunze¹, Ulrike Langematz¹, Stefanie Meul¹, Martine Michou⁶, Olaf Morgenstern⁷, and Luke D. Oman⁸

¹Institut für Meteorologie, Freie Universität Berlin, Berlin, Germany, ²Center for Atmosphere Ocean Science, Courant Institute of Mathematical Sciences, New York University, New York, USA, ³Center for Global Environmental Research, National Institute for Environmental Studies, Tsukuba, Japan, ⁴Senatsverwaltung für Stadtentwicklung und Umwelt, Berlin, Germany, ⁵Leibniz-Institut für Troposphärenforschung (TROPOS), Leipzig, Germany, ⁶GAME/CNRM, Météo-France, Centre National de Recherches Meteorologiques, Toulouse, France, ⁷National Institute of Water and Atmospheric Research, Wellington, New Zealand, ⁸Atmospheric Chemistry and Dynamics Laboratory, NASA Goddard Space Flight Center, Greenbelt, Maryland, USA

Abstract The meridional circulation of the stratosphere, or Brewer-Dobson circulation (BDC), is projected to accelerate with increasing greenhouse gas (GHG) concentrations. The acceleration is typically quantified by changes in the tropical upward mass flux (F_{trop}) across a given pressure surface. Simultaneously, models project a lifting of the entire atmospheric circulation in response to GHGs; notably, the tropopause rises about a kilometer over this century. In this study, it is shown that most of the BDC trend is associated with the rise in the circulation. Using a chemistry-climate model (CCM), F_{trop} trends across 100 hPa are contrasted with those across the tropopause: while F_{trop} at 100 hPa increases 1–2 %/decade, the mass flux entering the atmosphere above the tropopause actually decreases. Similar results are found for other CCMs, suggesting that changes in the BDC may better be described as an upward shift of the circulation, as opposed to an increase, with implications for the mechanism and stratosphere-troposphere exchange.

1. Introduction

The Brewer-Dobson circulation (BDC) characterizes the meridional transport of mass through the stratosphere. Air rises in the tropics and descends back into the troposphere in the extratropics of both hemispheres, primarily in the winter hemisphere. The BDC accelerates in response to increased greenhouse gas (GHG) forcing across a range of atmospheric models with varying representations of the stratosphere [e.g., Butchart, 2014, and references therein].

In concert with chemical processes, the BDC sets the distribution of trace gases throughout the stratosphere, notably ozone and water vapor. Changes in the stratospheric circulation can thus impact the surface. Butchart and Scaife [2001] highlight the impact of changes in the transport of both ozone and ozone depleting substances (ODSs), while Solomon et al. [2010] and Dessler et al. [2013] show the influence of stratospheric water vapor changes on surface temperature.

In models, the acceleration of the BDC is measured in terms of the residual mean circulation (RC) and typically quantified by the tropical upward mass flux (F_{trop}) across a fixed lower stratospheric pressure level, e.g., 70 or 100 hPa. Changes in the RC cannot be observed directly, as the meridional overturning in the stratosphere is 2 orders of magnitude smaller than in the troposphere. Indirect estimates are consistent with an acceleration of the overturning circulation [e.g., Young et al., 2012], but estimates of changes in the stratospheric age of air (AoA), a related but distinct measure of the overturning circulation based on observations of trace gases, do not reveal clear trends, if anything hinting at a deceleration of the BDC [e.g., Engel et al., 2009; Stiller et al., 2012].

Both observations and model simulations, however, show a clear upward shift of the tropopause with tropospheric warming and stratospheric cooling [Santer et al., 2003]. For the troposphere, an upward shift of the whole tropospheric circulation pattern is reported by Singh and O’Gorman [2012]. In the stratosphere, Shepherd and McLandress [2011] argue that GHG-induced tropospheric warming causes an upward displacement of the critical layers for wave breaking, allowing more wave activity to penetrate into the subtropical

lower stratosphere, thereby increasing—and lifting—the BDC. The strength of the meridional overturning decays markedly in height, so that a rise in the circulation will have a pronounced impact on the meridional overturning when measured at a fixed pressure level, even if the structure remains otherwise unchanged.

In this paper, we use the state-of-the-art chemistry-climate model (CCM) European Centre Hamburg (ECHAM)/Modular Earth Submodel System (MESSy) Atmospheric Chemistry (EMAC) to separate trends in the circulation associated with the lifting of the atmospheric circulation from other changes in the mass exchange between the troposphere and the stratosphere. We find that changes at a fixed pressure level are dominated by the lifting, and that mass transport in and out of the stratosphere changes comparatively little. A similar picture emerges from other models participating in the Chemistry-Climate Model Initiative (CCMI) [Hegglin and Lamarque, 2015], suggesting that changes in the BDC might better be described as a lifting of the overturning circulation than a structural increase in it. This provides a new perspective on the *Shepherd and McLandress* [2011] mechanism for the “increase” of the BDC and suggests that changes in stratosphere-troposphere exchange, which are important for tracer distributions and AoA based estimates, may be more subtle than the large changes in the RC measured at fixed pressure levels.

2. Models and Simulations

EMAC is a numerical chemistry and climate simulation system [Jöckel *et al.*, 2006], using the first version of the Modular Earth Submodel System to link multi-institutional codes, including homogeneous and heterogeneous chemical reactions (Module Efficiently Calculating the Chemistry of the Atmosphere, [Sander *et al.*, 2005]). The core atmospheric model is the fifth generation European Centre Hamburg (ECHAM5) general circulation model [Roeckner *et al.*, 2006]. We applied EMAC in the T42L39MA resolution, i.e., with a spherical truncation of T42 (corresponding to a grid of approximately $2.8^\circ \times 2.8^\circ$) with 39 hybrid pressure levels up to 0.01 hPa. The vertical spacing was chosen to carefully resolve the tropopause region, with levels at approximately 200, 170, 150, 130, 115, 100, 90, and 80 hPa.

Three atmosphere-only simulations were integrated for 141 years from 1960 to 2100, after at least 5 years of spin-up. The boundary conditions for the GHGs follow the Representative Concentration Pathway (RCP) scenarios 4.5, 6.0, and 8.5 [van Vuuren *et al.*, 2011], and the simulations are named *RCP4.5*, *RCP6.0*, and *RCP8.5*, accordingly. The specifications for the ODSs follow the scenario A1 from *World Meteorological Organization (WMO)* [2007]. Sea surface temperatures (SSTs) and sea ice concentrations (SICs) have been prescribed from scenario simulations performed with the Max Planck Institute Earth System Model (MPI-ESM) [Schmidt *et al.*, 2013] for the simulations *RCP4.5* and *RCP8.5* and from the Met Office Hadley Centre Earth System Model (HadGEM2-ES) [Jones *et al.*, 2011] for the simulation *RCP6.0*.

A fully coupled simulation, denoted *RCP6.0-O*, was integrated with the coupled atmosphere-ocean (AO) CCM EMAC-O, which comprises the EMAC model as described above coupled, via the Ocean Atmosphere Sea Ice Soil coupler [Valcke *et al.*, 2003], to the ocean model MPI-OM. This simulation has been performed from 1960 to 2096. The GHG and ODS specifications are the same as for the *RCP6.0* integration. The analysis of output from four additional CCMI models, detailed in Table 1, is included for comparison.

3. Tropical Upward Mass Flux With Respect to the Tropopause

The total tropical upward mass flux, F_{trop} , is computed by integrating the RC across the region of upwelling in the tropics. It is commonly used as an indicator for the strength of the BDC [e.g., Holton, 1990], and BDC changes are typically quantified by changes in F_{trop} across a fixed pressure level. Modeling studies almost universally project an increase in F_{trop} across pressure surfaces throughout the stratosphere with rising GHGs [e.g., Butchart and Scaife, 2001; Li *et al.*, 2008; McLandress and Shepherd, 2009; Butchart *et al.*, 2010; Okamoto *et al.*, 2011; Oberländer *et al.*, 2013; Bunzel and Schmidt, 2013].

Figure 1a shows the annual mean evolution of F_{trop} at 100 hPa from the EMAC simulations and ERA-Interim reanalysis data [Dee *et al.*, 2011]. We choose the 100 hPa level as it closely matches the tropical tropopause. For 1979–2013 all EMAC simulations correspond reasonably well with ERA-Interim data. While there is significant interannual variability in the mass flux, the well-established increase in F_{trop} in response to enhanced GHG forcing is projected in all simulations, the increase varying from 0.9 to 1.9 %/decade depending on the scenario. The strongest GHG scenario simulation (*RCP8.5*, red) and *RCP6.0-O* (green) show the largest

Table 1. Models and Model Simulations Used in This Study^a

Model	Reference	Chemistry	Ocean-SSTs/SICs	Simulations
EMAC	Jöckel et al. [2006]	Interactive chemistry in T + S	Prescribed from HadGEM2-ES (RCP6.0) and MPI-ESM (RCP4.5 and RCP8.5)	REF-C2 (RCP6.0), RCP4.5, RCP8.5
EMAC-O	Jöckel et al. [2006], Jungclaus et al. [2006], and Valcke et al. [2003]	Interactive chemistry in T + S	Coupled ocean model (MPI-OM)	REF-C2 (RCP6.0-O)
CCSRNIES- MIROC3.2	Imai et al. [2013]	Interactive chemistry in S	Prescribed from MIROC3.2	REF-C2
CNRM-CCM	Michou et al. [2011]	Interactive chemistry	Prescribed SSTs	REF-C2
GEOS-CCM	Oman and Douglass [2014]	Interactive chemistry in S	Prescribed from Community Earth System Model version 1 (CESM1)	Two realizations of REF-C2, ODSs: A1 2010 & A1 2014
Niwa-UKCA	Morgenstern et al. [2013]	Interactive chemistry	Coupled ocean model	REF-C2

^aAll REF-C2 simulations [Eyring et al., 2013] are based on the RCP6.0 scenario [van Vuuren et al., 2011]. The simulations are performed with either stratospheric (S) or tropospheric and stratospheric (T + S) chemistry included. The sea surface temperatures (SSTs) and sea ice concentrations (SICs) are previously generated from a coupled AO-GCM and prescribed to the CCM (EMAC, CCSRNIES-MIROC3.2, CNRM-CCM, and GEOS-CCM) or interactively generated by the coupled AO-CCM (EMAC-O and Niwa-UKCA).

increases. Enhanced warming in the tropics in the coupled simulation RCP6.0-O causes more acceleration compared to the atmosphere-only simulation RCP6.0 (not shown).

The tropopause is expected to rise in response to GHG-induced warming of the troposphere and cooling of the stratosphere [Held, 1982; Santer et al., 2003]. As shown in Figure 1c, all EMAC simulations project a substantial increase in the tropopause height, where the tropopause is identified using the standard lapse

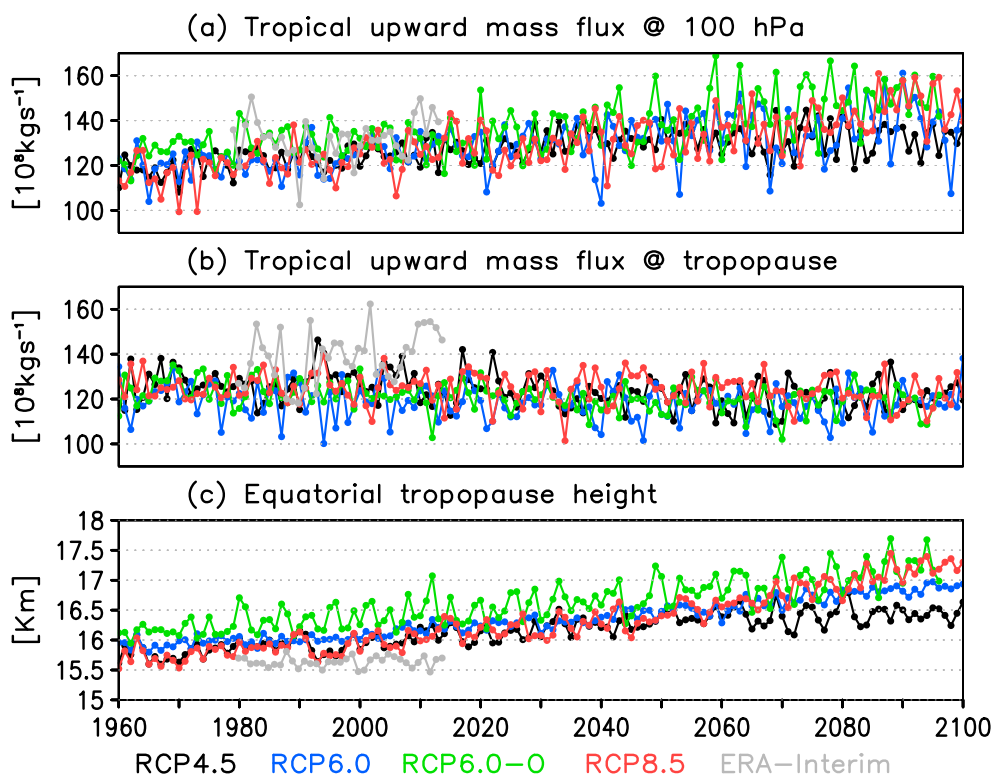


Figure 1. Time series of EMAC simulations RCP4.5 (black), RCP6.0 (blue), RCP6.0-O (green), and RCP8.5 (red) from 1960 to 2100 (1960–2096 for RCP6.0-O) and ERA-Interim data (grey) from 1979 to 2013 in the annual mean for (a) tropical upward mass flux at 100 hPa (10^8kg s^{-1}), (b) tropical upward mass flux at tropopause level (10^8kg s^{-1}), and (c) tropopause height at the equator (km).

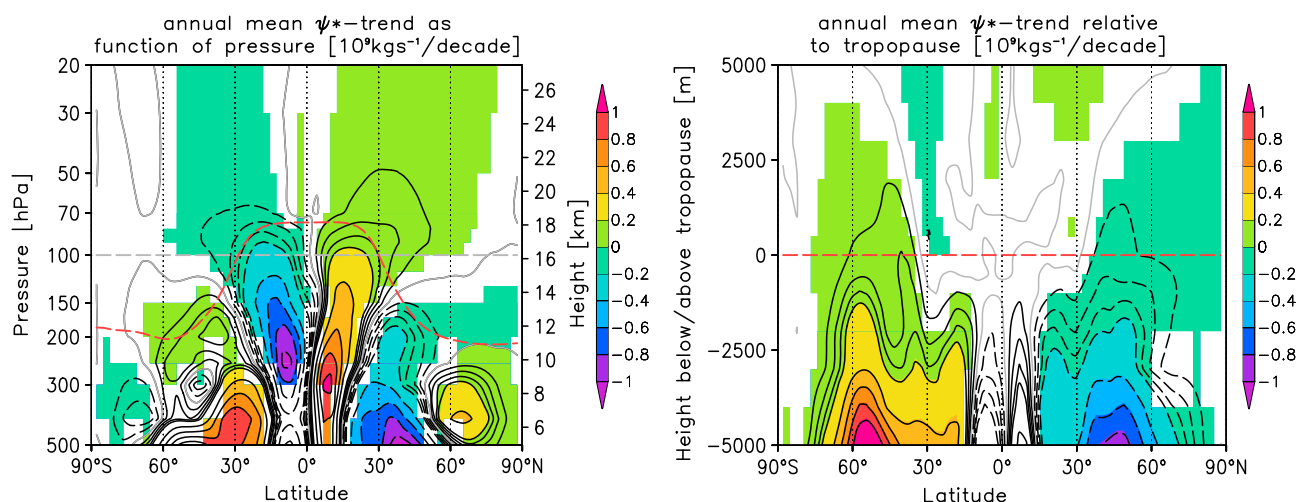


Figure 2. Annual mean linear trend in residual mean mass stream function (Ψ^*) between 1960 and 2096 for the simulation RCP6.0-O with respect to (left) pressure levels and to the (right) tropopause. Colored shading indicates statistical significance at the 95% level. The contours are $(\pm 0.05, 0.1, 0.15, 0.2, 0.4, 0.8, 1.0) \times 10^9 \text{ kg s}^{-1}/\text{decade}$ with solid lines indicating positive values (zero line in grey), and dashed lines negative values. The annual mean tropopause and the 100 hPa height for 1960 are included in dashed red and grey lines, respectively.

rate definition [WMO, 1957; Reichler *et al.*, 2003]. Given these large changes in the vertical structure of the atmosphere, we ask whether the change in F_{trop} at a fixed pressure level accurately describes changes in the transport of mass between the troposphere and the stratosphere. Figure 1b shows the time evolution of the tropical upward mass flux with respect to the tropopause for the EMAC simulations and ERA-Interim reanalysis. This is computed by integrating the mass flux exactly at the tropopause, adjusting the height as it rises in response to GHG increase. Between 1960–2000 and 2060–2100 (2096 for RCP6.0-O), F_{trop} at the tropopause actually *decreases*, with trends of -0.46 ± 0.33 , -0.20 ± 0.16 (-0.47 ± 0.30), and -0.26 ± 0.02 %/decade for the RCP4.5, RCP6.0 (RCP6.0-O), and RCP8.5 integrations.

To show the structure of the RC changes, Figure 2 illustrates the linear trend in the residual mean mass stream function, Ψ^* , for the coupled EMAC integration RCP6.0-O; a qualitatively similar picture emerges from the atmosphere-only integrations (not shown). The trend is computed in two ways, first with respect to pressure—as is the standard practice—and second, with respect to the tropopause. As in the calculations shown in Figure 1b, this is achieved by computing the tropopause at each time step, remapping the vertical coordinate relative to this level (denoted “0” in the plot) and then averaging. A similar procedure was applied by Birner [2006] to reveal the tropopause inversion layer, which is blurred out when averaged on pressure levels. More importantly for us, this procedure will also follow the tropopause upward as the atmospheric circulation responds to GHGs.

The Ψ^* trend exhibits a strikingly different structure depending on the averaging. When averaged on pressure surfaces (Figure 2a) the positive (clockwise) anomaly in the Northern Hemisphere and negative (counterclockwise) anomaly in the Southern Hemisphere indicate an acceleration of the circulation. When averaged with respect to the tropopause (Figure 2b), however, the Ψ^* trend reveals weak anomalies of opposite sign, characterizing a modest reduction in the RC at the tropopause in both hemispheres. From a physical point of view, when mapped relative to a fixed pressure level, changes are dominated by the upward expansion of the Hadley cell, which enhances the circulation in the tropics. But when mapped relative to the tropopause—which rises with the expanding Hadley cell—there are no significant changes in the tropics at all, and only a weak reduction in the extratropics.

4. The Effective Shift of the Measurement Level

The ascent of the atmospheric circulation in response to global warming implies that observations held at a fixed pressure level will effectively “see” a lower part of the atmosphere with time. For example, in the RCP6.0-O integration, the tropical tropopause shifts from 94.5 to 85.9 hPa from the last decade of the 20th century to the end of the 21st century. Thus, an analysis at 90 hPa would reveal significant changes in the chemistry and circulation related to the transition from the stratosphere to the troposphere.

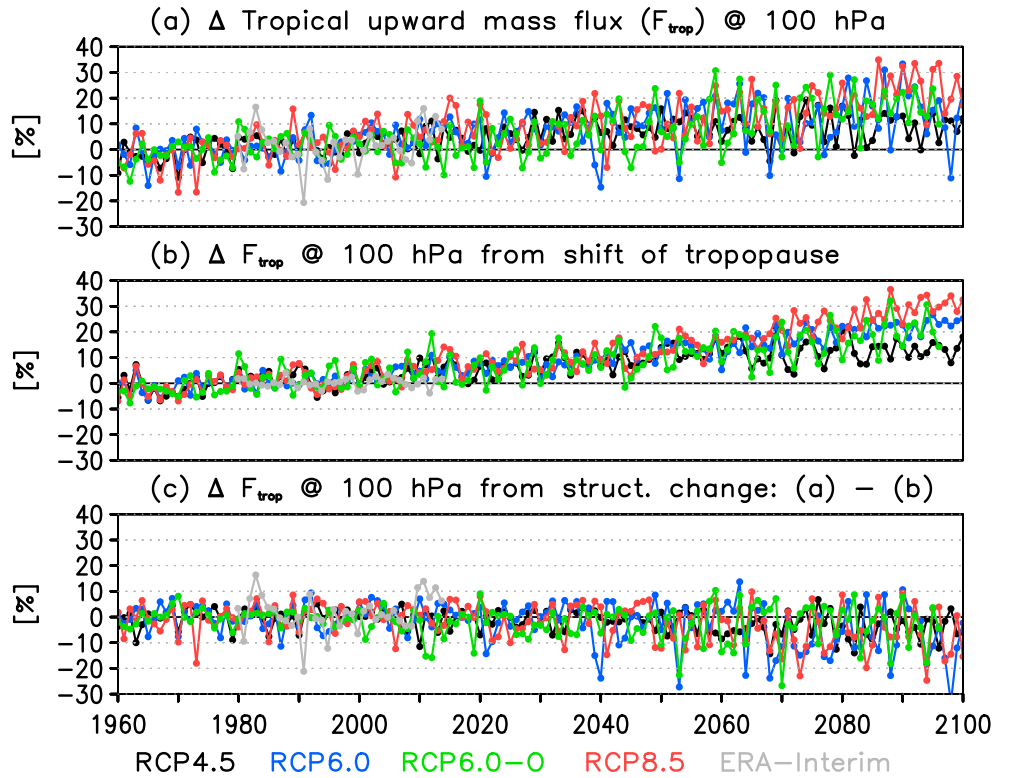


Figure 3. Annual mean change in tropical upward mass flux at 100 hPa of EMAC simulations RCP4.5 (black), RCP6.0 (blue), RCP6.0-O (green), and RCP8.5 (red) from 1960 to 2100 (1960–2096 for RCP6.0-O) and ERA-Interim data (grey) from 1979 to 2013 compared to the mean of the years 1960–2000 (ERA-Interim: 1979–2000) (%) for (a) total change (ΔF_{trop}), (b) change from shift of the tropopause (ΔF_{shift}), and (c) structural change (ΔF_{struct}) from Figures 3a and 3b.

Our goal is to separate the change in the tropical upward mass flux associated with the lifting of the circulation from other structural changes. The change in F_{trop} at a given pressure level, ΔF_{trop} , is decomposed into a change associated with the rise of the circulation, ΔF_{shift} , and other changes, ΔF_{struct} :

$$\Delta F_{\text{trop}} = \Delta F_{\text{shift}} + \Delta F_{\text{struct}}. \quad (1)$$

The change associated with an upward shift is estimated with a single term Taylor expansion, using the climatological vertical gradient of the mass flux from the historical period, $\left. \frac{\partial F_{\text{trop}}}{\partial z} \right|_{\text{past}}$, and the shift of the measurement level *relative to the circulation* between the future and past climates, Δz :

$$\Delta F_{\text{shift}} = \left. \frac{\partial F_{\text{trop}}}{\partial z} \right|_{\text{past}} \times \Delta z. \quad (2)$$

Note that both terms on the right-hand side of (2) will be negative: the mass circulation decays with height and a fixed pressure level will sink relative to the tropopause with time. We use the historical simulation to define the mass flux gradient in an effort to capture future circulation changes given only the trend in the tropopause. Lastly, ΔF_{struct} is defined as the difference between ΔF_{trop} and ΔF_{shift} .

Focussing on a specific lower stratospheric level, here 100 hPa, we estimate the vertical gradient in the mass flux with the closest levels above and below in the standard CCM output over the period 1960–2000:

$$\left. \frac{\partial F_{\text{trop}}}{\partial z} \right|_{\text{past}} = \frac{F_{\text{trop}}(115 \text{ hPa}) - F_{\text{trop}}(90 \text{ hPa})}{z(115 \text{ hPa}) - z(90 \text{ hPa})}. \quad (3)$$

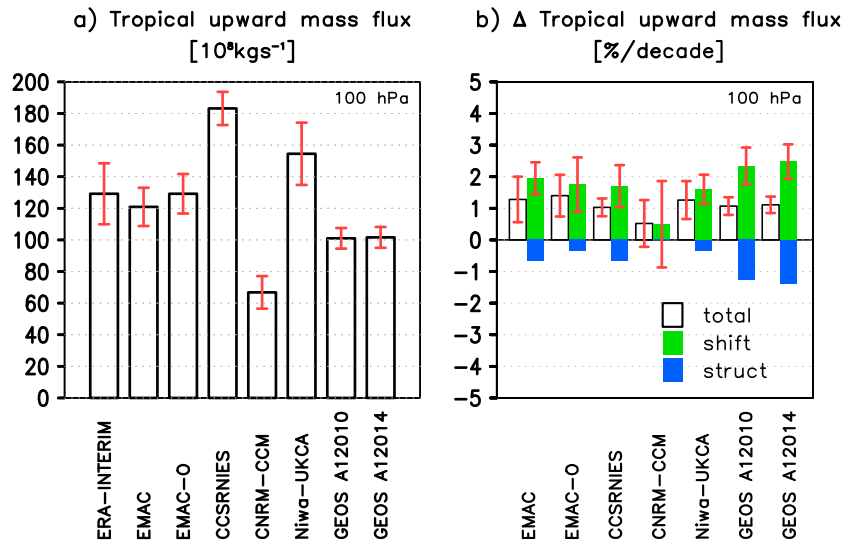


Figure 4. Climatology and changes in annual mean tropical upward mass flux at 100 hPa for the simulations under the RCP6.0 scenario from Table 1. (a) Annual mean F_{trop} averaged for the period 1960 to 2000 (CNRM-CCM: 1961 to 2000) (10^8 kg s^{-1}). For comparison climatological data as mean for the period 1979 to 2000 is added from ERA-Interim. (b) Changes in F_{trop} (white), F_{shift} (green), and F_{struct} (blue) between the periods 2060–2100 (2060–2096 for RCP6.0-O and 2060–2099 for CNRM-CCM and GEOS-CCM) and 1960–2000 (1961–2000 for CNRM-CCM) (%/decade). The red bars denote the uncertainties at the 95% confidence level. Note that coarser vertical resolution was available for the GEOS integrations, such that the decomposition likely suffers from larger truncation errors which are not accounted for in the uncertainty intervals.

We use the tropopause to quantify the shift of the circulation, so Δz is given by the change in the 100 hPa level relative to the tropopause:

$$\begin{aligned} \Delta z &= (z(100 \text{ hPa})|_{\text{future}} - z(\text{tropo})|_{\text{future}}) - (z(100 \text{ hPa})|_{\text{past}} - z(\text{tropo})|_{\text{past}}) \\ &= (z(\text{tropo})|_{\text{past}} - z(\text{tropo})|_{\text{future}}) + (z(100 \text{ hPa})|_{\text{future}} - z(100 \text{ hPa})|_{\text{past}}), \end{aligned} \quad (4)$$

with $z(\text{tropo})|_{\text{future}}$ and $z(\text{tropo})|_{\text{past}}$ referring to the tropopause height at the future and historical states. From the first term in (4), we see that Δz will be negative: as the tropopause rises, our effective measurement level is pushed lower in the atmosphere. The second term corrects for the fact that all pressure levels rise with tropospheric warming; it will always be smaller in magnitude than the first term if the pressure of the tropopause drops.

Figure 3a shows the relative change in F_{trop} at 100 hPa from EMAC as a function of time. As shown in previous studies, the RC increases substantially in response to GHG forcing. Figure 3b, however, shows that this increase can almost entirely be attributed to the effective change in the measurement level. It was obtained using equation (2), where the time evolution comes only from the shift in the 100 hPa surface relative to the tropopause, Δz .

ΔF_{struct} can be interpreted as an estimate of the change in the RC at the tropopause. Consistent with the analysis in the previous section, the residual “structural changes” in the mass flux, Figure 3c, are small and (if anything) negative. Notably, the structural term differs less between the different RCP scenarios, i.e., the impact of enhanced GHG forcing is felt through the rise in the circulation.

Figure 4 places EMAC in the context of other CCM1 models. There is substantial spread in the climatological RC; F_{trop} at 100 hPa ranges from ~ 70 to $180 \times 10^8 \text{ kg s}^{-1}$ (Figure 4a). All the models, however, project an increase in F_{trop} at 100 hPa under the RCP6.0 scenario forcing. When scaled relative to the climatological mass flux, most models are clustering around a rate of $\sim 1\%$ /decade (Figure 4b, white bars).

The green bars in Figure 4b show the change associated with the rise in the circulation: in all cases, the increasing F_{trop} trend at 100 hPa can largely be attributed to the rise of the tropopause relative to this pressure level. With the exception of CNRM-CCM, the shift term ΔF_{shift} is larger than the total change ΔF_{trop} , suggesting a weak reduction of the mass transport across the tropopause (Figure 4b, blue bars). In general, differences

between the models are comparable to the differences between the atmosphere-only and coupled EMAC integrations. These EMAC integrations differ at the lower boundary, suggesting that uncertainty in SSTs might explain the difference between models.

5. Discussion and Conclusions

A wide range of atmospheric and climate models robustly projected substantial changes in the BDC, almost uniformly quantifying trends by changes in the RC at fixed pressure levels. Our results are consistent with these previous studies but suggest a new interpretation. Given the lifting of the entire atmospheric circulation in response to GHG increase [Singh and O’Gorman, 2012], the stratosphere itself is changing substantially. When changes in tropopause height are taken into account, we find that the residual mean transport of mass between the troposphere and the stratosphere changes little in response to anthropogenic forcing, if anything decreasing slightly. Trends in the RC at a given pressure level can thus be simply linked to the effective descent of the pressure surface relative to the climatological overturning circulation.

This interpretation of the RC provides a new perspective on the mechanism. Shepherd and McLandress [2011] explain the RC change as a response to the upward movement of the zero wind line—a critical level for wave breaking of stationary waves—associated with the lifting of the subtropical jets. The conceptual model of Held [1982] predicts a vertical extension of the troposphere (and hence of the subtropical jets) in response to enhanced surface temperatures. Essentially, as the surface warms, the tropopause must rise in order to keep the atmosphere in radiative balance. Santer *et al.* [2003] demonstrate that a rising tropopause is a generic response of the atmosphere to changing GHGs. Our analysis suggests that an increase in the RC at a given pressure surface in the lower stratosphere may be equally generic. While models differ substantially in their ability to capture the meridional overturning of the stratosphere (e.g., Figure 4a), equation (2) implies that the relative change in F_{trop} depends largely on the shift of the tropopause. The CCMI models examined in this study predict a similar increase in tropopause height and thus a fairly uniform relative increase in the RC (Figure 4b).

We have focussed on the 100 hPa surface, given its proximity to the tropopause, but our approach can equally be applied to other surfaces. For example, the 70 hPa surface is often used as a benchmark for the strength of the RC. The EMAC-O integration projects an increase of 1.24 ± 0.60 %/decade at this level, consistent with other models [e.g., Butchart *et al.*, 2010]. In the twentieth century climatology of EMAC, 70 hPa is 1.71 km above the tropopause, but by the end of the century, it is only 1.16 km above the tropopause. This shift causes an F_{trop} increase of 1.29 ± 0.80 %/decade at 70 hPa.

While mass exchange between the stratosphere and the troposphere remains about constant in models, the ventilation of the stratosphere will change. The 10 hPa shift in the tropopause simulated by EMAC implies an approximately 10% reduction of the mass of the stratosphere. Neglecting the mixing of air along isentropic surfaces which cross the tropopause, the transit time of air through the stratosphere is given by its total mass, M , divided by the total mass exchange rate, F_{trop} . Hence, if the exchange rate remains about constant while M decreases, the mean transit time will decrease. Barring substantial changes in isentropic mixing, one would then expect the AoA to decrease. Based on an analysis of CCMs, Garny *et al.* [2014] suggest that the isentropic mixing may actually change predictably with the circulation and further reduce the AoA. Thus, our results do not resolve the mismatch of modeling studies with observational studies that find little evidence for a decrease in the AoA to date [Engel *et al.*, 2009; Stiller *et al.*, 2012].

References

- Birner, T. (2006), Fine-scale structure of the extratropical tropopause region, *J. Geophys. Res.*, *111*, D04104, doi:10.1029/2005JD006301.
- Bunzel, F., and H. Schmidt (2013), The Brewer-Dobson circulation in a changing climate: Impact of the model configuration, *J. Atmos. Sci.*, *70*, 1437–1455.
- Butchart, N. (2014), The Brewer-Dobson circulation, *Rev. Geophys.*, *52*, 157–184, doi:10.1002/2013RG000448.
- Butchart, N., and A. A. Scaife (2001), Removal of chlorofluorocarbons by increased mass exchange between the stratosphere and troposphere in a changing climate, *Nature*, *410*, 799–802.
- Butchart, N., *et al.* (2010), Chemistry-climate model simulations of twenty-first century stratospheric climate and circulation changes, *J. Clim.*, *23*, 5349–5374, doi:10.1175/2010JCLI3404.1.
- Dee, D. P., *et al.* (2011), The ERA-Interim reanalysis: Configuration and performance of the data assimilation system, *Q. J. R. Meteorol. Soc.*, *137*, 553–597, doi:10.1002/qj.828.
- Dessler, A. E., M. R. Schoeberl, T. Wang, S. M. Davis, and K. H. Rosenlof (2013), Stratospheric water vapor feedback, *Proc. Natl. Acad. Sci.*, *110*, 18087–18091, doi:10.1073/pnas.1310344110.

Acknowledgments

This work was supported by the DFG Research Unit FOR 1095 (SHARP) grants LA1025/13-2, LA1025/14-2, and LA1025/15-2, the DFG project ISOLAA (LA 1025/19-1), the BMBF MiKlip project (01LP1168A), the project StratoClim (603557), and the U.S. NSF (AGS-1264195). We thank the North-German Supercomputing Alliance (HLRN) and ECMWF computing center, the modeling groups, and the WCRP SPARC/IGAC CCMI for organizing and coordinating the model activity. O.M. acknowledges funding by the Royal Society Marsden Fund and by NIWA under its Government-funded, core research. NIES’ research was supported by the Environment Research and Technology Development Fund (2-1303) of the Ministry of the Environment, Japan. Data for this paper are available at the Freie Universität Berlin SHARP data archive under GRL_BDC_increase_or_shift_Oberlaender-Hayn_2015.tar.

- Engel, A., et al. (2009), Age of stratospheric air unchanged within uncertainties over the past 30 years, *Nat. Geosci.*, *2*, 28–31, doi:10.1038/ngeo388.
- Eyring, V., et al. (2013), Overview of IGAC/SPARC Chemistry-Climate Model Initiative (CCMI) community simulations in support of upcoming ozone and climate assessments, *SPARC Newslett.*, *40*, 48–66.
- Garny, H., T. Birner, H. Bönisch, and F. Bunzel (2014), The effects of mixing on age of air, *J. Geophys. Res. Atmos.*, *119*, 2034–2034, doi:10.1002/2013JD021417.
- Held, I. M. (1982), On the height of the tropopause and the static stability of the troposphere, *J. Atmos. Sci.*, *39*, 412–417, doi:10.1175/1520-0469(1982)039<0412:OTHOTT>2.0.CO;2.
- Hegglin, M. I., and J.-F. Lamarque (2015), The IGAC/SPARC Chemistry-Climate Model Initiative Phase-1 (CCMI-1) model data output. [Available at <http://catalogue.ceda.ac.uk/uuid/9cc6b94df0f4469d8066d69b5df879d5>.]
- Holton, J. R. (1990), On the global exchange of mass between the stratosphere and the troposphere, *J. Atmos. Sci.*, *47*(3), 392–395.
- Imai, K., et al. (2013), Validation of ozone data from the superconducting Submillimeter-Wave Limb-Emission Sounder (SMILES), *J. Geophys. Res. Atmos.*, *118*, 5750–5769, doi:10.1002/jgrd.50434.
- Jöckel, P., et al. (2006), The atmospheric chemistry general circulation model ECHAM5/MESy1: Consistent simulation of ozone from the surface to the mesosphere, *Atmos. Chem. Phys.*, *6*, 5067–5104, doi:10.5194/acp-6-5067-2006.
- Jones, C. D., et al. (2011), The HadGEM2-ES implementation of CMIP5 centennial simulations, *Geosci. Model Dev.*, *4*, 543–570, doi:10.5194/gmd-4-543-2011.
- Jungclaus, J. H., N. Keenlyside, M. Botzet, H. Haak, J.-J. Luo, M. Latif, J. Marotzke, U. Mikolajewicz, and E. Roeckner (2006), Ocean circulation and tropical variability in the coupled model ECHAM5/MPI-OM, *J. Clim.*, *19*, 3952–3972, doi:10.1175/JCLI3827.1.
- Li, F., J. Austin, and J. Wilson (2008), The strength of the Brewer-Dobson circulation in a changing climate: Coupled chemistry-climate model simulations, *J. Clim.*, *21*, 40–57, doi:10.1175/2007JCLI1663.1.
- McLandress, C., and T. G. Shepherd (2009), Simulated anthropogenic changes in the Brewer-Dobson circulation, including its extension to high latitudes, *J. Clim.*, *22*(6), 1516–1540, doi:10.1175/2008JCLI2679.1.
- Michou, M., et al. (2011), A new version of the CNRM chemistry-climate model, CNRM-CCM: Description and improvements from the CCMVal-2 simulations, *Geosci. Mod. Dev.*, *4*, 873–900, doi:10.5194/gmdd-4-1129-2011.
- Morgenstern, O., G. Zeng, N. L. Abraham, P. J. Telford, P. Braesicke, J. A. Pyle, S. C. Hardiman, F. M. O'Connor, and C. E. Johnson (2013), Impacts of climate change, ozone recovery, and increasing methane on surface ozone and the tropospheric oxidizing capacity, *J. Geophys. Res. Atmos.*, *118*, 1028–1041, doi:10.1029/2012JD018382.
- Oberländer, S., U. Langematz, and S. Meul (2013), Unraveling impact factors for future changes in the Brewer-Dobson circulation, *J. Geophys. Res. Atmos.*, *118*, 10,296–10,312, doi:10.1002/jgrd.50775.
- Okamoto, K., K. Sato, and H. Akiyoshi (2011), A study on the formation and trend of the BDC, *J. Geophys. Res.*, *116*, D10117, doi:10.1029/2010JD014953.
- Oman, L. D., and A. R. Douglass (2014), Improvements in total column ozone in GEOSCCM and comparisons with a new ozone-depleting substances scenario, *J. Geophys. Res. Atmos.*, *119*, 5613–5624, doi:10.1002/2014JD021590.
- Reichler, T., M. Dameris, and R. Sausen (2003), Determining the tropopause height from gridded data, *Geophys. Res. Lett.*, *30*(20), 2042, doi:10.1029/2003GL018240.
- Roeckner, E., R. Brokopf, M. Esch, M. Giorgetta, S. Hagemann, L. Kornblueh, E. Manzini, U. Schlese, and U. Schulzweida (2006), Sensitivity of simulated climate to horizontal and vertical resolution in the ECHAM5 atmosphere model, *J. Clim.*, *19*, 3771–3791.
- Sander, R., A. Kerkweg, P. Jöckel, and J. Lelieveld (2005), Technical note: The new comprehensive atmospheric chemistry module MECCA, *Atmos. Chem. Phys.*, *5*, 445–450, doi:10.5194/acp-5-445-2005.
- Santer, B. D., et al. (2003), Contributions of anthropogenic and natural forcing to recent tropopause height changes, *Science*, *301*(5632), 479–483, doi:10.1126/science.1084123.0.
- Schmidt, H., S. Rast, F. Bunzel, M. Esch, M. Giorgetta, S. Kinne, T. Krümler, G. Stenchikov, C. Timmreck, L. Tomassini, and M. Walz (2013), Response of the middle atmosphere to anthropogenic and natural forcings in the CMIP5 simulations with the Max Planck Institute Earth system model, *J. Adv. Model. Earth Syst.*, *5*, 98–116, doi:10.1002/jame.20014.
- Shepherd, T. G., and C. McLandress (2011), A robust mechanism for strengthening of the Brewer-Dobson circulation in response to climate change: Critical-layer control of subtropical wave breaking, *J. Atmos. Sci.*, *68*, 784–797, doi:10.1175/2010JAS3608.1.
- Singh, M. S., and P. A. O’Gorman (2012), Upward shift of the atmospheric general circulation under global warming: Theory and simulations, *J. Clim.*, *25*, 8259–8276, doi:10.1175/JCLI-D-11-00699.1.
- Solomon, S., K. H. Rosenlof, R. W. Portmann, J. S. Daniel, S. M. Davis, T. J. Sanford, and G.-K. Plattner (2010), Contributions of stratospheric water vapor to decadal changes in the rate of global warming, *Science*, *327*, 1219–1223.
- Stiller, G., et al. (2012), Observed temporal evolution of global mean age of stratospheric air for the 2002 to 2010 period, *Atmos. Chem. Phys.*, *12*, 3311–3331, doi:10.5194/acp-12-3311-2012.
- Valcke, S., A. Caubel, D. Declat, and L. Terray, (2003), OASIS3 Ocean Atmosphere Sea Ice Soil users’s guide, *Tech. Rep. TR/CMGC/03/69*, CERFACS, Toulouse, France.
- van Vuuren, D. P., et al. (2011), The representative concentration pathways: An overview, *Clim. Change*, *109*(1–2), 5–31, doi:10.1007/s10584-011-0148-z.
- World Meteorological Organization (WMO) (1957), *Meteorology a three-dimensional science: Second session of the commission for aerology*, WMO Bull. IV, Geneva, Switzerland.
- World Meteorological Organization (WMO) (2007), *Global Ozone Research and Monitoring Project-Rep. 50*, Geneva, Switzerland.
- Young, P. J., K. H. Rosenlof, S. Solomon, S. C. Sherwood, Q. Fu, and J.-F. Lamarque (2012), Changes in stratospheric temperatures and their implications for changes in the Brewer-Dobson circulation, 1979–2005, *J. Clim.*, *25*, 1759–1772, doi:10.1175/2011JCLI4048.1.